

Scramjet testing in high-enthalpy shock tunnel (HIEST)

Hideyuki TANNO, Katsuhiko ITOH, Syuichi UEDA,
Tomoyuki KOMURO, Kazuo SATO, Masatoshi KODERA
Ramjet Propulsion Research Center, *E-mail: tanno@kakuda-splab.go.jp*

Keywords: Scramjet, hypervelocity, shock tunnel, combustion, CFD, flight testing

1. Introduction

Scramjet has been studied for almost half a century because of its potential for space propulsion systems. However basic characteristics, such as its operational flight altitude and flight speed are still unknown. This is because it can operate at extremely high speeds of flight Mach number 8 or higher at which conventional wind tunnels are useless. Hence, experimental approaches have been restricted thus far. For scramjet ground testing under such high-speed conditions, NAL has modified a high-enthalpy shock tunnel (HIEST)¹⁾, which can produce test flow conditions of up to Mach number 25. Since 1999, NAL has been studying scramjet testing technology in the HIEST; (1) Development of a force measurement technique²⁾ for short test periods (2) Development of a fuel supply system³⁾ with a huge hydrogen flow rate. With these techniques and systems, scramjet testing in the HIEST was conducted.

This report describes the current status of NAL scramjet studies in the HIEST. Firstly, the results of the 2m-length NAL sub-scale scramjet tests conducted in the HIEST are shown. CFD analysis was also conducted.

Next, a new scramjet model designed for flight Mach number 12 conditions is described.

2. NAL sub-scale scramjet testing in HIEST

2.1 Purpose of testing

The NAL sub-scale scramjet combustion testing in the HIEST was conducted for the following two purposes: (1) Estimation of the accuracy of scramjet testing in the HIEST (2) Examination of scramjet performance in high-speed flow conditions. For the former purpose, comparison of HIEST results with blow-down wind tunnel (RJTF) results was conducted in the same flow conditions. For the latter purpose, stagnation enthalpy was varied from 4MJ/kg to 7.5MJ/kg, conditions equivalent to flight Mach number 7 to 13.

2.2 Experiment and CFD

A schematic diagram of the scramjet is shown in Figure 1. In the figure, x coordinate is the distance from the leading edge of the inlet. With side wall compression inlet and strut of 43mm thickness, the contraction ratio of the scramjet is 8.3.

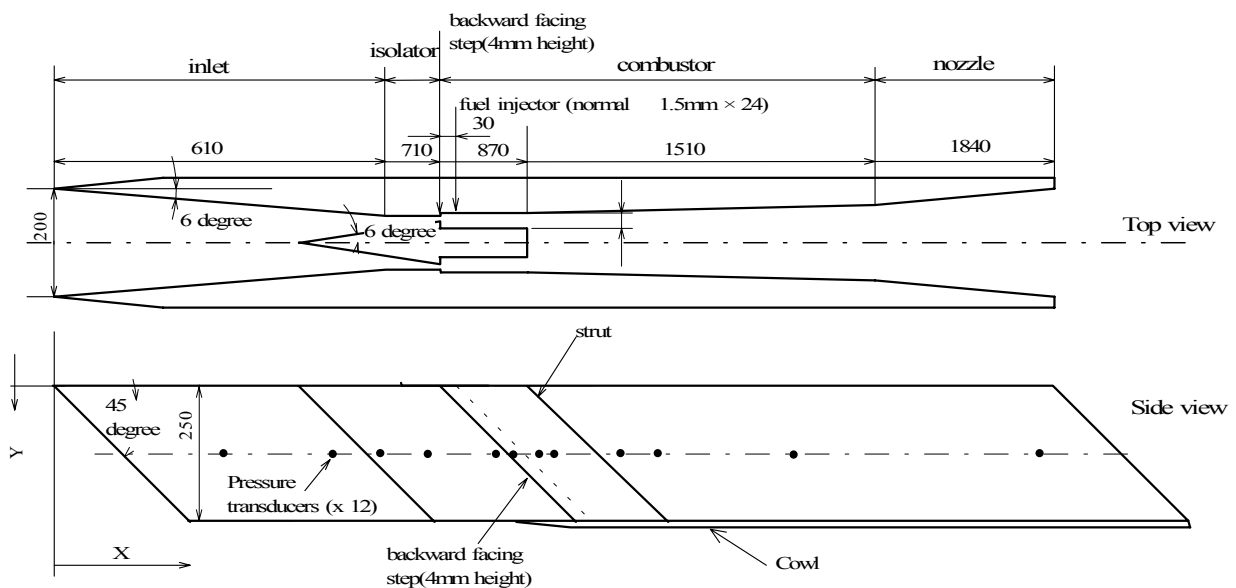


Figure.1 NAL sub-scale scramjet

Facility	HIEST				RJTF
Facility nozzle expansion ratio	256(Contoured $\approx 800\text{mm}$)				197.5(Square $510 \times 510\text{mm}$)
Test gas	Air/N ₂				Vitiated air
Flight Mach No.	7	8	10	13	8
P ₀ (MPa)	17	14	14	20	10
H ₀ (MJ/kg)	3.3	4	5.6	7.5	4
M	7.8	7.7	7.6	6.5	6.7
V (km/s)	2.4	2.6	3.1	3.6	2.6
T (K)	270	300	480	740	330
P (kPa)	1.6	1.5	1.3	2.2	1.6

Table.1 Test flow condition

Overall length and cross section of the inlet are 2.1m and 0.2 x 0.25m respectively. On

each sidewall, twelve fuel orifices of 1.5mm in diameter were placed the position of which is 30mm downstream from a backward-facing step of 4mm in height. Room temperature hydrogen sonic transverse injection was conducted through these orifices. The hydrogen mass flow was controlled with manifold pressure maintained at a constant level throughout the test period. To measure wall pressure and aerodynamic force, 41 pressure transducers and 13 accelerometers were mounted on the model. Drag force can be calculated from measured acceleration on the scramjet so the scramjet was suspended with four steel wires to enable it to move freely.

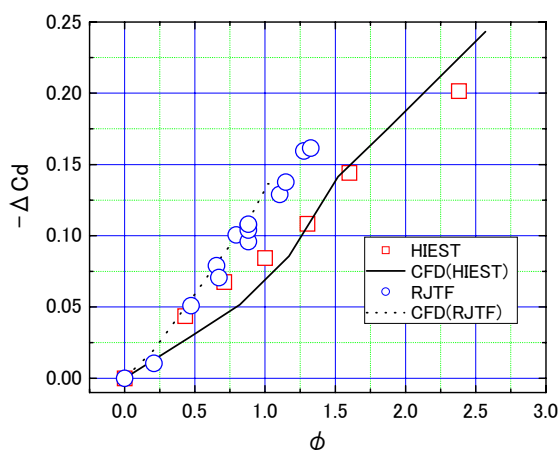
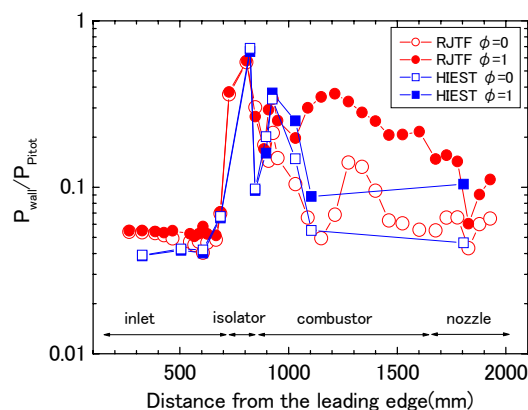


Figure.2 Drag reduction of the NAL sub-scale scramjet in HIEST and RJTF

For detailed investigation of the flow in the scramjet, numerical analysis was conducted to simulate scramjet flow in the RJTF and the

HIEST. The numerical code used in this study is a 3-D compressible reacting flow code⁴⁾ with an unstructured hybrid grid system. In the case of the RJTF, the boundary layer of the facility nozzle wall was ingested into the scramjet. Hence, the 87mm thickness of velocity profile of the 1/7-th power law was given as the top-wall boundary condition. Test flow conditions are shown in Table 1.

For comparison with the RJTF, stagnation pressure and stagnation enthalpy of the test flow was set to 14MPa and 4MJ/kg respectively adjusted to match flow condition of the RJTF testing.

Figure.3 Pressure distribution along the centerline on the side-wall($\phi=0, 1$)

For examination of the scramjet performance in high-speed conditions, stagnation enthalpy was varied from 3.3MJ/kg to 7.5MJ/kg which is equivalent to a flight Mach number of 7 to 13. From measured shock

speed in the shock tube and nozzle reservoir pressure, test flow condition was obtained by the non-equilibrium flow calculation code

NENZF. To change (fuel equivalence ratio) from 0 to 2.2, hydrogen manifold pressure was varied from 1.2MPa to 5.8MPa. In order to estimate the net thrust produced by combustion, testing with nitrogen test gas was also conducted.

2.3 omparison of Hiest and RJTF test results

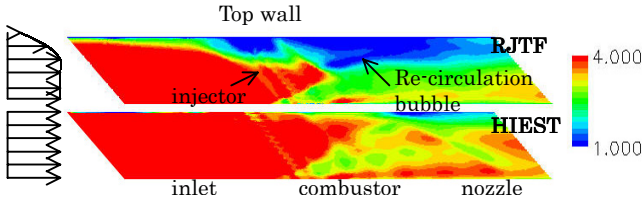


Figure.4 Mach number distribution in the scramjet in each facility simulated by CFD

Figure 2 shows drag reduction ($\Delta C_d = C_{d_{Air}} - C_{d_{N_2}}$) of the scramjet with different obtained in the RJTF and the Hiest. At $\gamma = 1.0$, drag reduction ΔC_d in the RJTF (-0.13) is larger than that in the Hiest (-0.08). It should be noted that the engine unstarted with $\gamma = 1.3$ in the RJTF whereas in the Hiest, ΔC_d continued to decrease with increased γ of up to 2.3. The ΔC_d difference between the RJTF and the Hiest was consistent with wall pressure difference in the scramjet. Figure 3 shows normalized side-wall pressure distribution of the scramjet in both facilities, distribution of which was obtained with $\gamma = 1.0$ and without hydrogen injection. The figure shows that pressure in the inlet, combustor and nozzle in the RJTF was higher than in the Hiest.

This difference can be related to the difference in the boundary layer profile between the RJTF and the Hiest. In the RJTF, the scramjet inlet was installed near the facility nozzle wall. Therefore on the top wall of the scramjet, a facility nozzle boundary layer of 87mm in thickness was ingested. This thick boundary layer caused a large separation on the top wall in the combustor. Figure 44 shows Mach number distribution in the scramjet, the distribution of which was obtained by numerical simulation in each of the facilities. The figure shows an obvious difference between the flow fields in the engines of each facility. In the RJTF, a large separation bubble was observed on the top wall, enhancing combustion meaning that wall pressure and measured C_d reduction was larger in the RJTF. In the Hiest, scramjet was tested in the core stream flow from the facility nozzle so that flow

in the engine is almost supersonic ($M > 2$) except wake near the downstream of the strut. There is therefore a thin boundary layer on the top wall. Consequently, small increases in pressure in the engine as well as smaller ΔC_d was observed in the Hiest. However, the engine does not unstart with $\gamma > 1.3$ in the Hiest.

2.4 Performance in high-speed flow conditions

Figure 5 shows drag reduction (net thrust) with different stagnation enthalpy. To estimate enthalpy effect on combustion, the ratio of hydrogen manifold pressure and free stream Pitot pressure ($P_{manifold}/P_{Pitot}$) was kept constant at approximately 30. Additionally, the effect produced by injection was subtracted by comparing the results of air test gas and nitrogen test gas. It is obvious that the thrust produced by combustion decreased with flow enthalpy.

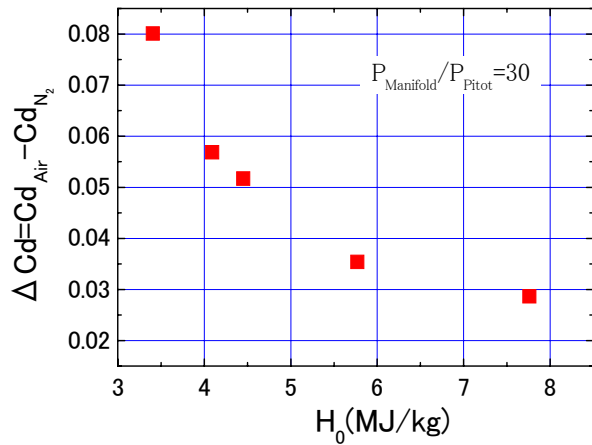


Figure.5 Effect of stagnation enthalpy on the net thrust($C_d = C_{d_{Air}} - C_{d_{N_2}}$)

3. New scramjet model designed for high-speed flow

In order to study the basic characteristics of high-speed combustion flow, a new scramjet model was designed under flight Mach number 12 conditions. To simplify the flow to the greatest extent possible, the scramjet was a rectangular duct with the side-wall compression shown in Figure 6.

The inlet angle was designed so as not to cause shock wave-boundary layer interaction on the inlet wall. To increase thrust, the combustor

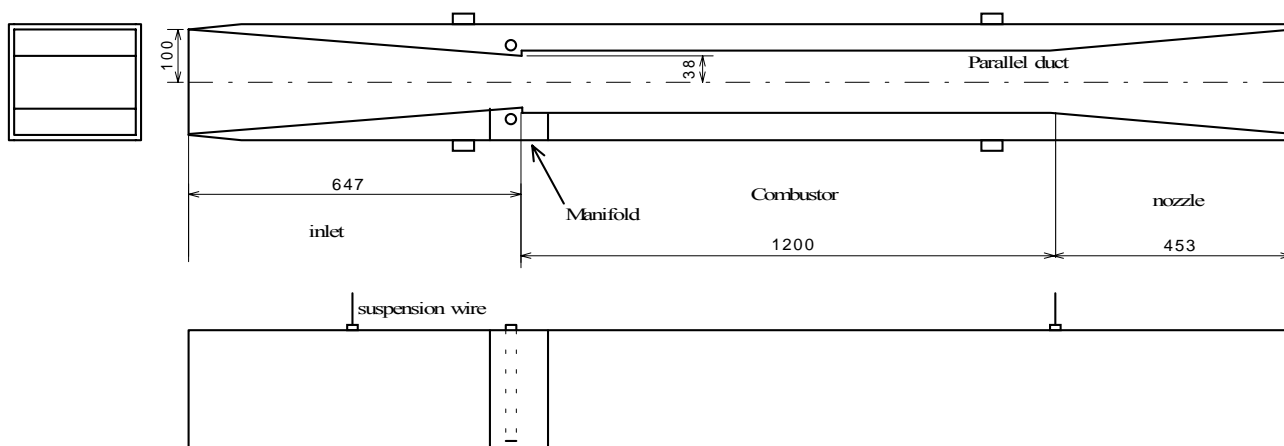


Figure.6 Schematics of M12 scramjet model

inflow temperature was as low as possible and the auto-ignition limit required inflow temperature of more than 900K. Hence, the inflow temperature was set to 1000K. Inflow pressure of the combustor was decided by the empirical rule proposed by Stalker⁵⁾. In his rule, production of pressure and combustor length has to be more than $24\text{kPa} \cdot \text{m}$ for combustion. Since maximum combustor length is limited to 1.2m for the present Hiest test section, pressure was determined to be 20kPa. For the temperature and pressure described above, inlet angle was designed to be 5.5 degrees. Moreover, inlet length was designed so that the leading edge shock did not attach to the inlet wall and so as not to cause shock wave– boundary layer interaction. Since the transverse injector may cause serious loss from bow shock initiated by injection, the parallel injector was designed to mitigate the flow perturbation. Mixing of fuel and air flow stream is not good for parallel injection, so a hyper mixer was thus designed to enhance air-fuel mixing. Stagnation pressure was adjusted to 40MPa, determined by a designed pressure of 24kPa with the present contoured nozzle.

Figure 7 shows pressure contour obtained by numerical simulation under designed conditions. The figure shows pressure increase caused by combustion occurring at the end of the

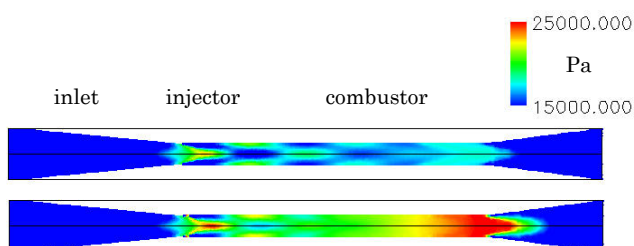


Figure.7 Pressure contour(Top: no inection, bottom: =1)

combustor meaning design seems reasonable.

4. Summary

The current status of scramjet research in high-speed flow conditions in the Hiest has been described. By comparison of the testing results obtained in the RJTF and the Hiest, the difference in the two facilities can be explained by the test flow non-uniformity caused by the facility nozzle boundary layer. These results demonstrate that 2m-length scramjet combustion testing can be conducted in the Hiest. Additionally, a new scramjet model was designed for basic study of high-speed flow conditions. The model will be tested in 2002.

Reference

- [1] ITOH K et. al. (1999) Hypervelocity aero-thermodynamic and propulsion research using a high-enthalpy shock tunnel (HIES). AIAA-99-4961.
- [2] TAKAHASHI M et. al. (1999) Development of a New Force measurement method WWW c for scramjet testing in a high-enthalpy shock tunnel. AIAA 99-4961.
- [3] TANNON H et. al. (2000) Fuel injection system for scramjet test in a large impulsive facility. ISTS 20000-a-15
- [4] KODERA M et. al. (2000) Numerical study of mixing and combustion process of a scramjet engine model. AIAA 00-0886
- [5] Stalker RJ and Paul A (2001) Scramjet and shock tunnels. ISABE 2001-1006